Research Article Vol. 34, No. 2 / 26 Jan 2026 / Optics Express 1510
Optics EXPRESS

Intrinsic distributed sensing using wavelength-multiplexed QPSK signals in fiber-optic communication

GEORGE Y. CHEN,[1,2] RUNLONG ZHU,[1,2] XING RAO,[1,2] JUNMIN LIU,[3] ZHIXIANG DENG,[4] SHUQING CHEN,[4] AND YIPING WANG[1,2,*]

[1]State Key Laboratory of Radio Frequency Heterogeneous Integration, Key Laboratory of Optoelectronic Devices and Systems of Ministry of Education and Guangdong Province, College of Physics and Optoelectronic Engineering, Shenzhen University, Shenzhen 518060, Guangdong Province, China
[2]Shenzhen Key Laboratory of Ultrafast Laser Micro/Nano Manufacturing, Guangdong and Hong Kong Joint Research Centre for Optical Fibre Sensors, Shenzhen University, Shenzhen 518060, Guangdong Province, China
[3]College of New Materials and New Energies, Shenzhen Technology University, Shenzhen 5l8118, China
[4]Institute of Microscale Optoelectronics, Shenzhen University, Shenzhen 5l8060, China
*ypwang@szu.edu.cn

Abstract: The integration between fiber-optic communication and sensing has gained enormous interest worldwide due to the potential for utilizing existing communication cable infrastructure for low cost structural-health monitoring and security applications. Forward distributed acoustic sensing is particularly promising for such integration, as the sensing and communication signals co-propagate, and grants advantages including long sensing distance, high sensitivity and wide frequency response. In this work, an integrated architecture is proposed and experimentally demonstrated for unidirectional fiber-optic communication and distributed sensing, which solves the detector synchronization problem that has hindered practical application. The sensing demodulator is separated from the communication demodulator by choice, in order to address practical deployment requirements regarding a closed-source commercial communication system and data security. The adoption of the self-referencing forward interferometry scheme improves optical stability, streamlines design and reduces cost. As demonstration, a quadrature phase-shift keying (QPSK) communication signal at a 1 Gbps modulation rate is multiplexed onto the optical carrier, with a transmission fiber length of ~90 km. The experimental results show that enabling the communication modulation does not cause significant degradation in sensing performance. The system demonstrated a sensitivity of 0.83 rad/V at 50 MHz, facilitating high-frequency ultrasonic detection in the 1MHz–50 MHz range, with a spatial resolution of 0.64 m at 5 MHz. This integrated architecture enables distributed sensing within the existing framework of communications while providing a means for data security, does not occupy additional bandwidth, and has the potential to unlock massively scalable sensing solutions.

1. Introduction

In recent years, distributed optical fiber sensing technology has made significant progress with innovations in system design, demodulation algorithms, specialty fibers and artificial intelligence [1]. This class of technologies enable real-time and continuous monitoring of physical quantities such as temperature, stress and vibration along the optical fiber, thereby facilitating disturbance detection in scenarios such as bridges, tunnels, railways, geological activities, and perimeter fences [2–5]. Optical frequency domain reflectometry (OFDR) is often used for high spatial resolution over short distances [6]. Phase-sensitive optical time-domain reflectometry (φ-OTDR,

#584647 https://doi.org/10.1364/OE.584647
Journal © 2026 Received 13 Nov 2025; revised 26 Dec 2025; accepted 26 Dec 2025; published 12 Jan 2026

Optics EXPRESS

also known as distributed acoustic sensing or DAS) focuses on application scenarios with medium distance and medium spatial resolution [7,8]. Without the use of optical amplifiers, its maximum sensing distance can typically only reach tens of kilometers. In practical applications, these techniques utilize narrow-linewidth lasers or swept-frequency lasers, which significantly increases the cost of the system This significantly limits the versatility and usage. However, leveraging existing optical fiber resources can lead to more practical solutions.

To date, the deployed fiber network of optical communications is very widespread and mature, with billions of kilometers laid globally including 1.4 million km undersea for transoceanic telecommunications. Therefore, as a cost-effective solution to meet the needs of the global information network, the integration between distributed sensing and communication has broad prospects and is, to a certain extent, an inevitable trend.

Forward transmission-based distributed sensing, or forward DAS, due to the forward transmission nature, is an emerging group of sensing technologies [9,10] that are fundamentally different from conventional backscattering-based measurement methods. Its nature of optical propagation is the same as that of optical communication, and thus existing fiber-optic communication systems and cable networks can be used without hardware modifications. In addition, the built-in distributed sensing function has no impact on transmission quality and does not occupy additional bandwidth. Forward DAS inherently possess, longer single-span sensing distance, high sensitivity, wider frequency response range and lower computation load.

Multiple demodulation schemes for forward DAS have been reported, including intensity [11], phase [12,13] and polarization [14]. Some research teams have demonstrated ultra-long multi-span sensing distances of up to thousands of kilometers using existing undersea communication cables and repeaters [15–17]. However, the sensing system in these demonstrations either cannot locate disturbances or lack analysis on the impact of sensing on data transmission. Ezra Ip et al. reported 489 km transmission experiments with a single-span sensing range of 53.9 km, and positioning accuracy of about 5 km [18]. However, the sensing aspect lacked true distributed sensing ability because it can only measure one perturbation point at a time. It should be noted that most forward DAS systems use a folded double-ended configuration, in order to avoid detector synchronization problems. However, when using a communication framework, a fiber loop is no longer possible, which adds an additional layer of complexity. The unidirectional forward sensing structure proposed by Qingming Chen et al. [19] used multiple wavelengths and the chromatic dispersion of the optical fiber for positioning, thus solving the problem of time synchronization of the demodulation ends. However, the architecture requires a reference arm with the same length as the sensing arm for interference, which increases the complexity of the system. We reported an integrated structure for communication and sensing previously. However, the two demodulation ends of the structure were located in separate places, rendering it difficult to achieve high-precision time/data synchronization [20].

In response to the significant demand and key challenges of the efficient utilization and intelligent upgrade of existing fiber-optic communication systems to support distributed sensing, we propose unidirectional communication-sensing integration based on dispersion for positioning. In this work, we show that the sensing aspect in the system can reuse the communication optical path, quadrature phase shift keying (QPSK) code modulation scheme, and successfully demonstrate multi-point disturbance positioning without synchronization nor data security issues. In addition, a study is carried out on the influence of communication on sensing. The research results provide validation for integration between fiber-optic communication (QPSK) and forward DAS, which can lead to a large-scale upgrade of transoceanic information networks.

2. Experiment design

In the proposed system, the optical communication infrastructure is directly used as the sensing system, with the data transmission forming the carrier for sensing (instead of steady power/phase).

Optics EXPRESS

The added sensing aspect has virtually no impact on the data transmission quality. Although perturbations from the external environment acts on the optical fiber and affects the quality of data transmission, the sensing aspect only analyzes a copy of the optical data at the receiving end, thus it neither interferes with communication nor occupies additional bandwidth. It is worth noting that externally induced noise is an inherent component in data transmission, and related issues have already been addressed in existing communication systems.

Figure 1 shows the layout of the integrated communication and sensing system. After the laser output is modulated by a pair of QPSK modulators, the communication data is encoded onto the optical carrier and transmitted along the optical fiber. When the optical signal is disturbed by the external environment, additional low-frequency modulations are superimposed on the phase, intensity, and polarization state of the carrier. At the detection stage, digital signal processing can effectively separate the communication data and the disturbance signal in the frequency domain, enabling independent processing of each function in each communication/sensing module. Based on the analysis of the detected disturbance signal, key information such as the disturbance amplitude, frequency, and occurrence position along the fiber can be accurately extracted. Due to data security requirements and the need to integrate with a proprietary, closed-source communication system, the sensing demodulator was deliberately designed to be separate from the communication demodulator. The sensing system does not require high-bandwidth hardware for demodulation. The sensing bandwidth only needs to exceed the maximum frequency of the disturbance signals, not necessarily match that of the high-capacity communication system. In practice, a low-pass filter can be implemented just before the sensing demodulator to remove communication data.

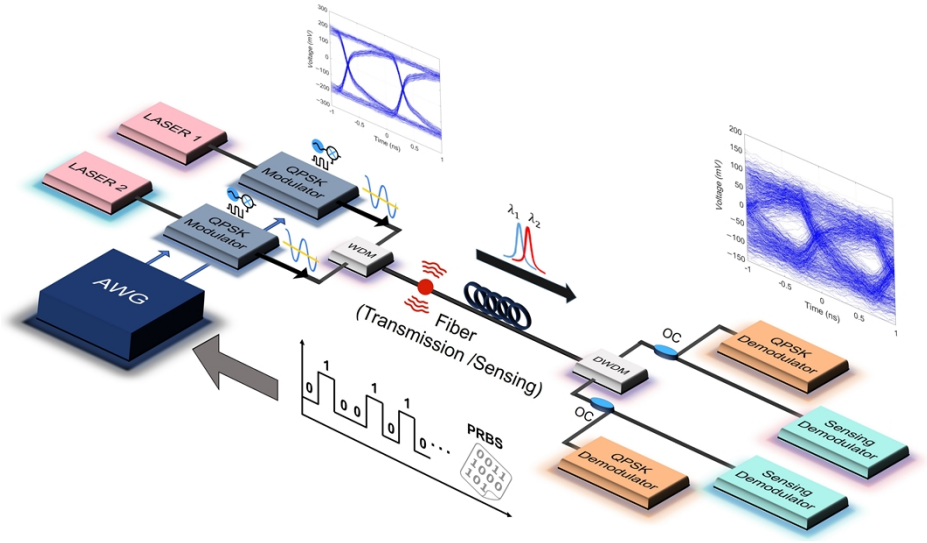

Fig. 1. Communication-sensing integrated system structure.

In the experiment, lasers that can emit wavelengths of C59 and C21 were chosen, which are commonly used in communication systems. Their wavelengths are 1530.334 nm (195.9 THz) and 1560.606 nm (192.1 THz) respectively. To ensure the consistency of the phase demodulation results, the specifications of the two laser sources should be as consistent as possible. Therefore, two same-brand tunable lasers were used, and the two wavelengths were chosen as far apart as possible within their adjustable wavelength range (1530-1565 nm) to improve the delay-induced spatial resolution. If the wavelength difference is too small, the time delay between the pair of phase signals may be too small to measure. If the difference is too large, lasers with different

Optics EXPRESS

specifications would be needed, which could result in different signal and noise characteristics. The power emitted by each laser is 6 dBm and the laser linewidth is 100 kHz. The main sources of phase noise in our experiments are the laser frequency drift and environmental factors, rather than laser power. Thus, increasing the laser power beyond 6 dBm would not have a significant improvement on the SNR and BER metrics. Instead, it would likely lead to various nonlinear effects that are detrimental to the performance of both sensing and communication systems. In the experiment, the modulator at the transmission end and the connectors of the optical path caused significant optical loss. Hence, we used 6 dBm laser power to ensure that the optical power entering the transmission/sensing fiber is greater than 1 dBm, which from experience is adequate for detection while avoiding significant nonlinear effects. The total length of the optical fiber is 89.85 km. For the purpose of demonstration, and the limitations of the experimental condition, only the C21 wavelength is modulated by QPSK with a bit rate of 1 Gbps. It is combined with the C59 wavelength through a wavelength division multiplexer (WDM) and injected into the transmission optical fiber. Different types of signals generated by an arbitrary waveform generator (AWG) are used to drive an electro-optic modulator (EOM) for simulating external disturbances acting on the optical fiber. A phase modulator is used instead of the usual piezoelectric ceramic (PZT) in order to probe the high-frequency response of the sensing system. High-frequency signals are often overlooked, which can be associated with dielectric breakdown of submarine cable coating under high voltage [21].

At the end of the transmission optical fiber, the two wavelengths enter the corresponding demodulation ends through a demultiplexer. After wavelength channel separation, the optical signal is split into two paths by a coupler. One path enters the QPSK demodulator (local laser as LO), while the other enters the sensing demodulator (delayed self-reference for LO). The self-referencing interferometry improves optical stability, streamlines design and reduces cost (does not need narrow laser linewidth nor a swept-frequency laser, which greatly reduces the cost). The sensing demodulator uses a 90° optical hybrid for interference, then a pair of balanced photodetectors (BPDs) for detection, and an oscilloscope for signal acquisition and processing. In the experiment, the bandwidth of the BPD utilized is 400 MHz, while that of the oscilloscope is 3 GHz. The sampling rate of the 4-channel oscilloscope was set to 625 MSa/s. Overall, the frequency response consistency, SNR and dynamic range of the self-referencing method are lower than those of the heterodyne interference method. However, the self-referencing method is less sensitive to environmental factors, has a simpler structure, and is generally more cost-effective than the heterodyne interference method.

The demodulation process is presented in Fig. 2. It is worth noting that to the sensing aspect, the communication data is a form of noise, and vice versa. The actual demodulated phase φ_s is the sum of the phase generated by disturbances, the encoded data, and laser frequency drift or phase noise. In the system, 30 m delay fibers are used at both demodulation ends. When the frequency of the laser drifts, the phase change caused by interference can be expressed by $\Delta\varphi = 2\pi\Delta f \frac{nL}{C}$. Where Δf represents the magnitude of the frequency drift, n represents the effective index of the delay fiber, and L represents the length of the delay fiber. The extent of frequency-induced phase drift can be estimated by analyzing the measured phase spectrum with both the disturbance and communication signals turned off. When the SNR (signal-to-noise ratio) is sufficiently high (e.g. >10), the phase noise of the laser generally does not affect the normal operation of the sensing system. In particular, the phase noise does not affect the sensitivity (mainly dependent on fiber material) but the limit of detection (this work focuses on the communication-sensing impact). Although it was not possible to compare the phase amplitudes of the communication and sensing signals at either detection module due to the difference in bandwidth/bandpass selection, it is possible to assess the noise contribution from communication modulation on the sensing signal. For example, at 5 MHz, the amplitude of the disturbance signal is 2.2216 rad, while that of the phase noise is only 0.0453 rad. On the other hand, the impact of the disturbance on the

Optics EXPRESS

communication signal can be made negligible due to bandpass filtering.

$$\varphi_s = \varphi_{vibration} + \varphi_{communication} + \varphi_{drift} \tag{1}$$

The sensing aspect is the main focus of this work, and thus the following section is dedicated to recovering the disturbance signal. The fast Fourier transform (FFT) is performed on the demodulated phase signal, and the main frequencies of the disturbance is determined by frequency analysis. Bandpass filtering is applied to the region where disturbances likely occur, prior to extracting the relevant frequency components.

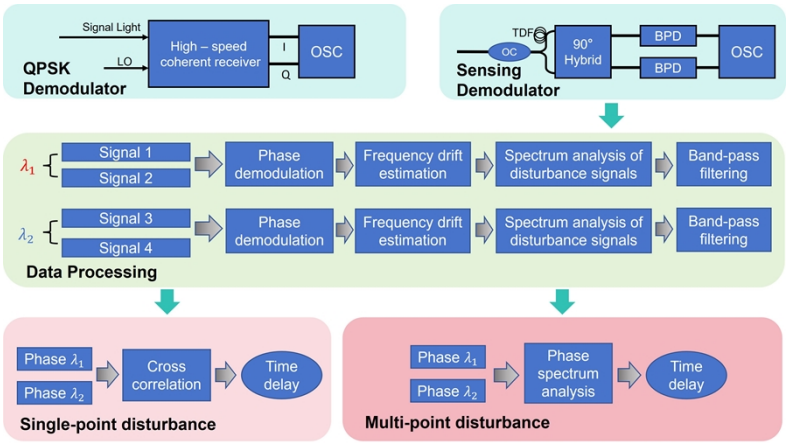

Fig. 2. Integrated system signal processing flow diagram.

In the proposed method, chromatic dispersion between two wavelengths of light is the underlying principle behind disturbance positioning. For single-mode optical fibers, it can be expressed as:

$$D_m(\lambda) = -\frac{\lambda}{c}\frac{d^2n}{d\lambda^2} \tag{2}$$

where n is the refractive index of the medium, λ is the wavelength of the light, and c is the speed of light in vacuum. For different wavelengths, the refractive index varies, which results in different transmission speeds of light in the optical fiber and different time of arrival for the same signal at the detection end. Therefore, knowing the time delay as a function of position along the fiber, the disturbance position L_{vib} can be inferred:

$$L_{vib} = \frac{\Delta t}{D_m \cdot (\lambda_1 - \lambda_2)} \tag{3}$$

where D_m is the dispersion coefficient in the 1550 nm band of single-mode fiber, and its value is approximately 17 ps/(nm·km). λ_1 and λ_2 represent the central wavelengths of the two wavelength channels. The aim of disturbance positioning is to resolve the time delay (Δt) between the phase signals of the two wavelengths.

When a single point of disturbance occurs along the optical fiber path, the time delay between the two signals can be determined by using the cross-correlation algorithm. When disturbances occur at multiple points on the optical fiber, it is necessary to use the phase spectrum [22] to measure the time delay between frequency components of the two wavelengths. The data processing flow of the phase-spectrum method is shown in Fig. 3.

Optics EXPRESS

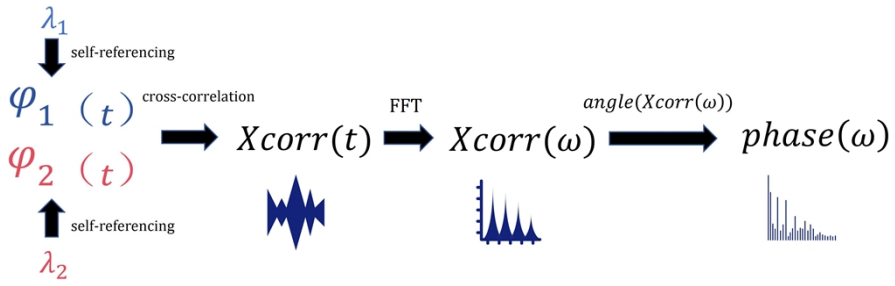

Fig. 3. The data-processing flow of the phase-spectrum method

One approach is to carry the cross-correlation between the two signals first, then apply FFT. The time delay between different frequencies can be expressed as:

$$t(\omega) = \frac{phase(\omega)}{\omega} \tag{4}$$

where ω is the radial frequency, being the frequency of the signal f multiplied by 2π. This method supports the detection of multiple disturbances, as long as their central frequencies are distinct and there are no overlaps.

3. Experiment results

3.1. Single-point perturbation test

The following series of experiments are designed to showcase the sensing performance under a single disturbance, as well as the impact of communication on the sensing metrics. The disturbance source was positioned at 70 km away from the demodulation end (verified using a commercial OTDR). The tested signal was a 5 MHz sine wave. Measurement of low-frequency signals is possible, though it requires data collection for a relatively long time at a high sampling rate to ensure that multiple periods of the signal are included. This would result in a very large amount of data. For the sake of computational efficiency and being constrained by limited computing power, only high-frequency signals were tested. Figure 4(a) and Fig. 4(d) show the phase waveforms when the modulation and demodulation functions of the communication signal were turned on and off. The laser source lacks a high-precision wavelength-stabilizing mechanism. The observed phase oscillation is likely caused by the laser source itself, and temperature-induced cavity effects produce a commonly observed oscillating behavior in the frequency and phase of light. Since the phase signal demodulated from the modulation of the communication signal has a certain degree of distortion. By locally magnifying the signal, the phase changes caused by the interference of the electro-optic modulator (EOM) can be observed. The situations when the modulation of the communication signal was turned on and off are shown in Fig. 4(b) and Fig. 4(e) respectively. From the FFT spectra shown in Fig. 4(c) and Fig. 4(f), it can be known that the disturbed signal is 5 MHz. From the Fourier transform spectrum, it can be seen that there are multiple frequency harmonics terms of the original signal. The QPSK signal affects the positioning accuracy to some extent. Some low-frequency components of the communication signal could superimpose on the vibration frequency components, and thus filtering might not fully remove them. However, for long-distance applications the current positioning accuracy is sufficient. By finding the peak of the Fourier spectrum, the frequency of the disturbance signal can be determined. After performing band-pass filtering on the phase signal, the cross-correlation algorithm can be used to obtain the time delay between the two wavelengths at this time, which is 27.44 ns (67.32 km).

Optics EXPRESS

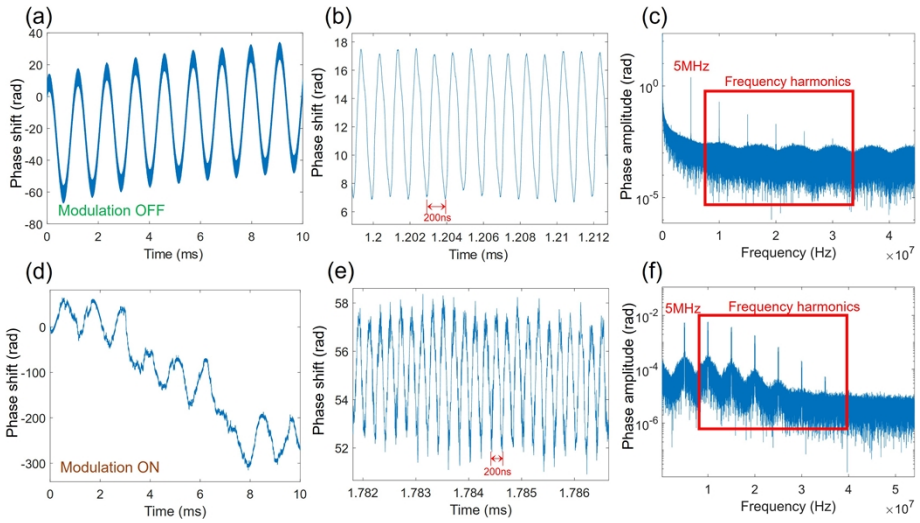

Fig. 4. Single-point distributed disturbance measurement: (a) Time-domain phase signal with modulation off; (b) Magnified phase signal with modulation off; (c) Fourier amplitude spectrum with modulation off. (d) Phase signal with modulation on; (e) Magnified phase signal with modulation on; (f) Fourier amplitude spectrum with modulation on.

The eye diagram of the communication signals for the cases where the disturbance is turned on/off in shown Fig. 5. Since the frequency range of the disturbance is much lower than the transmission rate of the communication signals, the impact of the disturbance on the communication signal is very limited. It can be observed that the voltage difference between the two levels dropped from 86 mV to 55 mV after the disturbance was activated. No bandpass filtering was applied for demonstration.

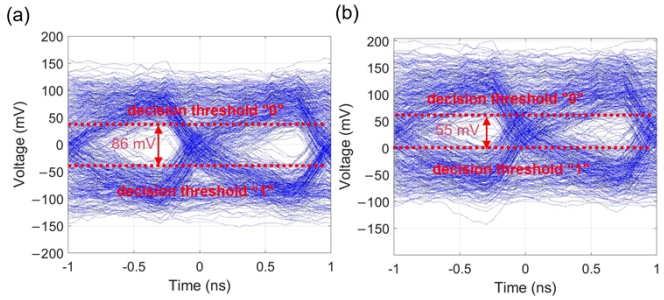

Fig. 5. The communication eye diagram: (a) when the disturbance signal is turned off; (b) when the disturbance signal is turned on.

In previous reports [19], the fiber dispersion coefficient is approximately 17 ps/(nm·km). To obtain a more accurate value specific to the optical fiber used in this system, disturbance sources were activated at positions of 20 km, 40 km, 50 km, 70 km and 90 km and 10 measurements were carried out at each position with the communication signal turned off to determine the dispersion coefficient. The corresponding time delay at each position were obtained using cross-correlation, as shown in Fig. 6. Using the gradient of the linear fitting, as the wavelength difference between the two beams of light is 30.272 nm, the dispersion coefficient of the fiber under test was calculated to be 16.4 ps/(nm·km) via Eq. (2). It is worth noting that a deviation of the positioning results was observed, which led to a baseline shift of 5.82 ns in the fitted curve.

Optics EXPRESS

Theoretically, itis caused the wavelength-dependency of the EOM. Hence, when calculating the position of the disturbance through the time delay, a correction of 5.82 ns is implemented.

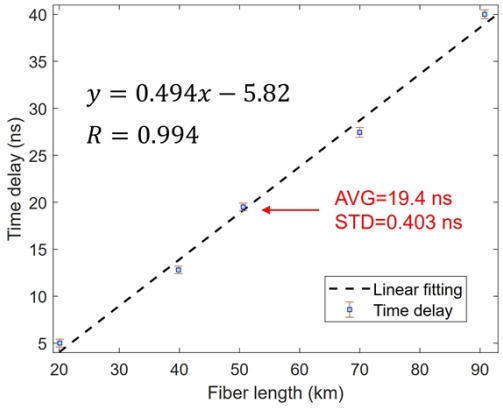

Fig. 6. Chromatic dispersion-induced time delay as a function of fiber length.

In order to understand the impact communication (seen as noise to the sensing aspect) has on the time delay, the modulation of the QPSK was added, and the positioning experiment was repeated for single-point disturbance under the same conditions. The disturbance source was situated at a position 50 km away from the receiving end. The positioning results at different disturbance frequencies and the test results of the time delay are shown in Table 1. Positioning accuracy refers to the standard deviation of the positioning results corresponding to the standard deviation of multiple time-delay measurement results. Sensitivity describes the rate of change between detected parameter and measurand, such as the change in phase shift caused by a unit change in vibration amplitude. Positioning error is the deviation between the mean positioning result and the true position. According to the lack of trend in the tested frequency range, the sensitivity shows no tendency to decline as the disturbance frequency increases. It can be seen that since the high-frequency communication signal introduces low-order frequency components that overlap with the disturbance signal to some extent, the standard deviation of the measured time delays has increased. When a 5 MHz disturbance occurs, the standard deviation of the time delay increases from 0.403 ns (when the communication signal is off, shown in Fig. 6) to 0.544 ns. The positioning accuracy can be as small as 0.99 km and the positioning error as small as 0.64 km. However, the overall positioning results are consistent with the fitting results in the absence of a communication signal.

Table 1. Time delay and sensitivity as a function of disturbance frequency.

Frequency (MHz)	Time delay (ns)	STD (ns)	Positioning accuracy (km)	Sensitivity (rad/V)	Positioning error (km)
1	19.2	0.548	1.11	0.80	0.64
5	20.0	0.544	1.10	0.72	2.26
10	19.2	0.448	0.99	0.78	0.64
30	19.2	0.596	1.20	0.74	0.64
50	18.4	0.560	1.13	0.83	-0.98

It is worth noting that according to the fitting results, when the disturbance occurs at a distance of 0 km from the demodulation end, the expected time delay is not zero. This is because when

Optics EXPRESS

the EOM modulates two wavelengths through refractive index modulation, it affects the initial phase of these two wavelengths differently.

3.2. Multi-point perturbation test

The positioning method involving phase-spectrum time delay was employed in the multi-point disturbance test. This time, EOMs were placed at positions of 70 km and 20 km away from the receiving end. Then, disturbances of 5 MHz and 9 MHz were respectively applied to these two EOMs to simulate ultra-high-frequency disturbances occurring at different positions simultaneously. The demodulated phase signal is presented in Fig. 7(a). The reason why the two signals are not identical is that the phase modulation characteristics of the two wavelengths in the two EOMs operating at 5 MHz and 9 MHz are inconsistent. At a result, the detected phase change of wavelength 1 is 0.965 rad at 5 MHz and 0.372 rad at 9 MHz, while that of wavelength 2 is 0.695 rad at 5 MHz and 0.694 rad at 9 MHz. This is caused by the wavelength-dependency and polarization-dependency of the EOMs, with the latter resulting from the different propagation speeds between the two wavelengths (chromatic dispersion) causing modulation to act on different states of polarization. The noise floor is maintained below 0.0085 rad, which is taken from the average phase noise amplitude at the signal frequency when the disturbance signal was turned off, and the measured sensitivity is 0.8 rad/V. It can be observed in Fig. 7(b) that there are two distinct frequency components. Since the sensing signals are affected by the communication "noise", a bandpass filter was applied before computing the phase spectrum of the signal. The phase can be converted into time-delay spectrum shown in Fig. 7(c), which are 29.7 ns and 5.2 ns, respectively, as shown in Fig. 7(d) and Fig. 7(e). The corresponding distances are 71.54 km and 22.19 km, respectively. Applying the previously calibrated relationship between time delay and position, the position errors are 1.57 km and 2.00 km, respectively. The errors presented here may have multiple sources. For example, the dispersion coefficient was assumed to be uniform throughout the fiber, which serves as the basis for positioning. In reality, different sections of the fiber could possess slightly different dispersion coefficients due to manufacturing process. The two laser sources may experience different levels of frequency drift, which can also cause fluctuations in the detected phase waveforms used for comparison. In addition, the state of polarization between the two wavelength channels are also likely to be different, which contributes to the interference process and thus affects the phase waveforms. The positioning accuracy (standard deviation of measured position values) also depends on the above factors, especially the frequency drift and state of polarization. In addition, the two laser sources did not have a phase-locking module, resulting in different initial phases, which may lead to phase drifts over time.The limitations of the algorithm's adaptability also exacerbate the positioning error to some extent. The high-efficiency cross-correlation algorithm proposed by [23], may overcome the limitations of traditional cross-correlation.

In the experiment, the sampling rate is 625 MSa/s, and the acquisition duration of each measurement is 1 ms. It should be noted that the positioning method using the phase spectrum is significantly different from the conventional cross-correlation method. The spatial resolution of the cross-correlation approach depends on the sampling rate. According to Eq. (3), the spatial resolution is 3.2 km. On the other hand, the spatial resolution of the phase-spectrum time-delay positioning method depends on the number of collected datapoints and the signal frequency. The time resolution is $dt = \frac{1}{Nf}$ .Where N represents the number of datapoints, and f denotes the signal frequency. For the 5 MHz disturbance signal, the number of datapoints is 625,000. Hence, the time resolution is 0.32 ps, and the corresponding spatial resolution is 0.64 m. The theoretical spatial resolution is calculated based on the fundamental principles, which is impossible to demonstrate in the experiment due to the fact that positions are taken from the middle point of the affected fiber regions, with fiber lengths far exceeding the spatial resolution. Comparing 3.2 km and 0.64 m, it is clear that the phase-spectrum method can greatly improve

Optics EXPRESS

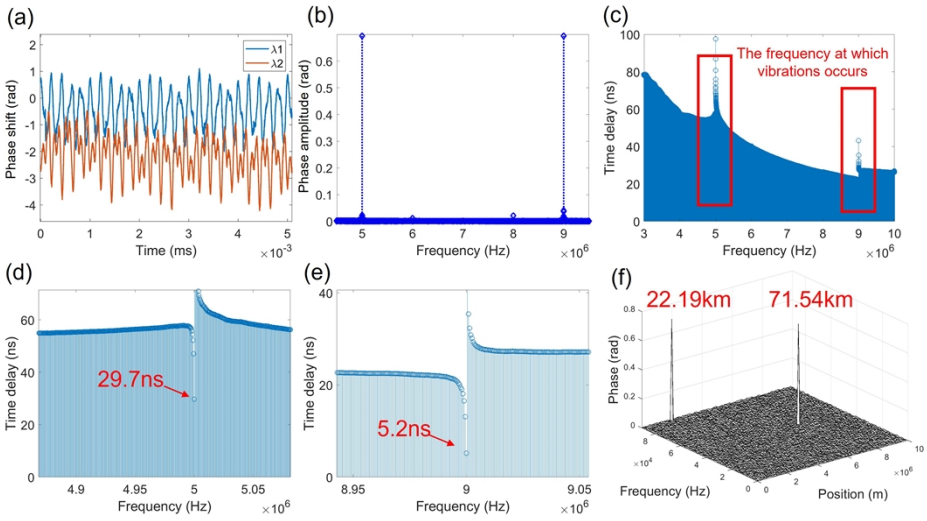

Fig. 7. Multi-point distributed disturbance measurement (modulation on): (a) Time-domain phase signal; (b) Fourier amplitude spectrum; (c) Magnified areas showing disturbance frequencies; (d) Disturbance 1 induced time delay (5 MHz); (e) Disturbance 2 induced time delay (9 MHz); (f) 3D plotting of the positioning results.

the spatial resolution of the sensing system when the number of datapoints is sufficient. However, increasing the number of datapoints will eventually reac0 h a tradeoff between spatial resolution and computation power. Positioning tests were also conducted on higher frequency signals up to 50 MHz. The SNR and sensitivity remain consistent, demonstrating the robustness of the system. In practical engineering, we may also encounter situations where the frequencies of multiple disturbance points are close or overlapping. In such cases, it will be difficult for the phase spectrum method to distinguish these disturbance points. The cepstrum method [23] is a promising approach to solve this problem, which can resolve multiple signals of the same frequency band, either single- or multi-frequencies. However, its signal processing is much more complex than that of the phase-spectrum method.

4. Conclusion

We reported an integrated architecture between a fiber-optic communication system using QPSK-encoded data transmission, wavelength-division multiplexing, and a forward transmission distributed fiber-optic disturbance sensor based on the chromatic dispersion for positioning and self-referencing interferometry for streamlined demodulation. Both functions are realized through the QPSK communication system without sensing taking up additional communication bandwidth. The sensor and communication demodulators are separate by design to meet deployment requirements for a closed-source commercial system and to ensure data security. When the communication data was transmitted at a rate of 1 Gbps, no significant impact was observed on the sensing performance metrics. Due to the bandwidth limitation (400 MHz) of the BPD used in the sensing demodulation process, even if a higher-rate communication signal is used, bandwidth-filtering means higher frequency components of communication will not affect the sensing performance. The single-span sensing distance is approximately 90 km, the spatial resolution is 0.64 m @ 5 MHz, the average sensitivity at 50 MHz is 0.83 rad/V, and the tested disturbance frequency range is from 1 MHz to 50 MHz. The positioning accuracy can be as small as 0.99 km and the positioning error as small as 0.64 km. This proof-of-concept demonstration reveals that the deep integration between communication and distributed sensing

Optics EXPRESS

based on self-referencing forward interferometry and chromatic dispersion is feasible. This system is more suitable for high-frequency disturbance signals due to the self-referencing design (simplicity) and fast-time sampling scheme. Only MHz signals were tested in the experiment. This is because for high-frequency signals (e.g., MHz), even short time delays such as 20 ns produces distinct phase characteristics, creating a sharp peak in cross-correlation. However, for low-frequency signals (e.g., kHz), the same time difference is negligible relative to the long period, making phase differences indistinct. To ensure algorithm performance, a high sampling rate is necessary, which can lead to high data volumes with extended measurement durations. If the measurement duration is too short to cover multiple periods, cross-correlation could fail to produce a clear peak. Compressive sensing is being explored to address this issue.

It is worth noting that some legacy optical communication networks still use dispersion compensation hardware modules. The method presented in this paper will not work in such systems. In systems where only algorithms are used for dispersion compensation, disturbance positioning needs to be carried out before the dispersion compensation stage. In addition, the system has the potential to be integrated with multiple erbium-doped fiber amplifiers (EDFAs) to form an ultra-long-distance communication-sensing integrated system. Although the amplified spontaneous emission (ASE) noise in the amplifiers may have a certain impact on the system, one can use methods such as optical filters or deep learning models to suppress the ASE noise and further improve the positioning accuracy of the system.

Funding. National Natural Science Foundation of China (W2532046, 62275172, U22A2088); Shenzhen Science and Technology Program (JCYJ20241202124408012, JCYJ20220818095800001); Shenzhen Science and Technology Program (ZDSYS20220606100405013); Scientific Instrument Developing Program of Shenzhen University (2023YQ027); Research Team Cultivation Program of Shenzhen University (2023DFT001).

Disclosures. The authors declare no conflicts of interest.

Data availability. Data underlying the results presented in this paper are not publicly available at this time but maybe obtained from the authors upon reasonable request.

References

1. P. Lu, N. Lalam, M. Badar, *et al.*, "Distributed optical fiber sensing: Review and perspective," Appl. Phys. Rev. **6**(4), 041302 (2019).
2. N. J. Lindsey, E. R. Martin, D. S. Dreger, *et al.*, "Fiber-Optic Network Observations of Earthquake Wavefields," Geophys. Res. Lett. **44**(23), 11792–11799 (2017).
3. D. Milne, A. Masoudi, E. Ferro, *et al.*, "An analysis of railway track behaviour based on distributed optical fibre acoustic sensing," Mechanical Systems and Signal Processing **142**, 106769 (2020).
4. J. Rodet, B. Tauzin, M. Amin Panah, *et al.*, "Urban dark fiber distributed acoustic sensing for bridge monitoring," Structural Health Monitoring-an International Journal **24**(1), 636–653 (2025).
5. H.-H. Zhu, D.-Y. Wang, B. Shi, *et al.*, "Performance monitoring of a curved shield tunnel during adjacent excavations using a fiber optic nervous sensing system," Tunnelling and Underground Space Technology **124**, 104483 (2022).
6. L. Ren, T. Jiang, Z.-g. Jia, *et al.*, "Pipeline corrosion and leakage monitoring based on the distributed optical fiber sensing technology," Measurement **122**, 57–65 (2018).
7. X. Li, Y. Zeng, N. D. Muchiri, *et al.*, "The use of distributed acoustic sensing (DAS) in monitoring the integrity of cement-casing system," Journal of Petroleum Science and Engineering **208**, 109690 (2022).
8. L.-Y. Shao, S. Liu, S. Bandyopadhyay, *et al.*, "Data-Driven Distributed Optical Vibration Sensors: A Review," IEEE Sens. J. **20**(12), 6224–6239 (2020).
9. Z. Wu, Z. Wu, and A. Sun, "Long distance distributed optical fiber vibration sensing and positioning technology based on loop transmission polarization detection," Measurement **225**, 114029 (2024).
10. Y. Yan, F. N. Khan, B. Zhou, *et al.*, "Forward Transmission Based Ultra-Long Distributed Vibration Sensing With Wide Frequency Response," J. Lightwave Technol. **39**(7), 2241–2249 (2021).
11. Y. Luo, L. Xia, D. Huang, *et al.*, "Quasi-Distributed Strain Sensing System Based on Optical Spectrum-Limited Chaos and CFBG Intensity Demodulation," IEEE Photonics J. **7**(1), 1–7 (2015).
12. Y. Li, Y. Wang, L. Xiao, *et al.*, "Phase Demodulation Methods for Optical Fiber Vibration Sensing System: A Review," IEEE Sens. J. **22**(3), 1842–1866 (2022).
13. G. Wang, Z. Pang, B. Zhang, *et al.*, "Time shifting deviation method enhanced laser interferometry: ultrahigh precision localizing of traffic vibration using a urban fiber link," Photonics Res. **10**(2), 433–443 (2022).
14. A. Mecozzi, M. Cantono, J. C. Castellanos, *et al.*, "Polarization sensing using submarine optical cables," Optica **8**(6), 788–795 (2021).

Optics EXPRESS

15. G. Marra, C. Clivati, R. Luckett, *et al.*, "Ultrastable laser interferometry for earthquake detection with terrestrial and submarine cables," Science **361**(6401), 486–490 (2018).
16. G. Marra, D. M. Fairweather, V. Kamalov, *et al.*, "Optical interferometry-based array of seafloor environmental sensors using a transoceanic submarine cable," Science **376**(6595), 874–879 (2022).
17. Z. Zhan, M. Cantono, V. Kamalov, *et al.*, "Optical polarization-based seismic and water wave sensing on transoceanic cables," Science **371**(6532), 931–936 (2021).
18. E. Ip, Y.-K. Huang, G. Wellbrock, *et al.*, "Vibration Detection and Localization Using Modified Digital Coherent Telecom Transponders," J. Lightwave Technol. **40**(5), 1472–1482 (2022).
19. Q. Chen, C. Jin, Y. Bao, *et al.*, "A distributed fiber vibration sensor utilizing dispersion induced walk-off effect in a unidirectional Mach-Zehnder interferometer," Opt. Express **22**(3), 2167–2173 (2014).
20. R. Zhu, X. Rao, S. Dai, *et al.*, "Deep Integration of Fiber-Optic Communication and Sensing Systems Using Forward-Transmission Distributed Vibration Sensing and on-off Keying," Sensors **24**(17), 5758 (2024).
21. Z. Sun, K. Liu, J. Jiang, *et al.*, "Distributed vibration sensing with high frequency response by using WDM based integrated scheme," J. Phys. D: Appl. Phys. **53**(15), 155106 (2020).
22. X. Rao, S. Dai, M. Chen, *et al.*, "Multi-point vibration positioning method for long-distance forward transmission distributed vibration sensing," Opt. Express **32**(17), 30775–30786 (2024).
23. Y. Chang, Q. Liu, H. Li, *et al.*, "High-efficiency cross-correlation algorithm for optical frequency domain reflectometry distributed sensing," Opt. Lett. **50**(16), 5026–5029 (2025).